



The Iron, Silicon and Oxygen Abundance in the Solar Wind Measured with SOHO/CELIAS/MTOF

P. Wurz¹, M. R. Aellig¹, F. M. Ipavich², S. Hefti^{1,6}, P. Bochsler¹, A. B. Galvin^{2,7}, H. Grünwaldt³, M. Hilchenbach³, F. Gliem⁴ and D. Hovestadt⁵

¹University of Bern, Physics Institute, CH-3012 Bern, Switzerland

²University of Maryland, College Park, MD 20742, U.S.A.

³Max-Planck-Institut für Aeronomie, D-37189 Katlenburg-Lindau, Germany

⁴Technische Universität Braunschweig, D-38023 Braunschweig, Germany

⁵Max-Planck-Institut für Extraterrestrische Physik, D-85740, Garching, Germany

⁶Present address: University of Michigan, Ann Arbor, MI 48109, U.S.A.

⁷Present address: University of New Hampshire, Durham, NH 03824, U.S.A.

Received 25 August 1998; revised 12 October 1998; accepted 20 October 1998

Abstract. From data collected with the MTOF sensor of the CELIAS instrument on board the SOHO spacecraft we derived the elemental abundance ratios for Si/O and Fe/O in the solar wind with high time resolution. Since Si and Fe are elements with a low first ionization potential (FIP) and oxygen is a high FIP element, these abundance ratios are valuable diagnostic tools for the study of the FIP fractionation process. The abundance ratios we find for slow and fast solar wind are commensurate with published values for interstream and coronal hole type solar wind. Between these two extreme cases of solar wind flow we find a continuous decrease of the abundance ratios for increasing solar wind speed, from a high value indicative of solar wind originating from the streamer belt to low values associated with flow from coronal holes.

© 1999 Elsevier Science Ltd. All rights reserved.

1 Introduction

In the solar wind, elements with low first ionization potential (below about 10 eV) are systematically enriched relative to high FIP elements compared to their photospheric abundance. The enrichment amounts to a factor of 3–5 for slow solar wind associated with the streamer belt, and about two for fast solar wind associated with coronal holes (von Steiger, 1996). It is generally believed that these relative enrichments are the result of a fractionation process taking place in the upper chromosphere and lower transition zone and are caused by a neutral-ion separation process, with the ionization most likely caused by the EUV radiation from the solar corona. Geiss and Bochsler (1986) found that the fractionation pattern of the elements is even better described using the first ionization time as the organizing parameter instead of the FIP. Several models have been designed to explain the FIP effect and have recently been reviewed by von Steiger (1996). So far none of these models is able to self-consistently explain the FIP effect. Recently, Peter (1996) extended the diffusion model put forward by Marsch et al. (1995) by intro-

ducing a chromospheric mass flow speed whose magnitude determines the strength of the FIP fractionation. We will compare our data with predictions derived from this model.

In this paper we report on the investigation of the oxygen, silicon, and iron densities in the solar wind, which often serve as a reference for the less abundant minor ions. Silicon and iron are low FIP elements and their abundance relative to oxygen, a high FIP element, will allow us to make conclusions on the FIP fractionation effect for different solar wind regimes. The data were gathered with the MTOF sensor of the CELIAS instrument (Hovestadt et al., 1995) on the SOHO mission. The SOHO spacecraft is located at the Lagrangian point L1 and is a three-axis stabilized spacecraft pointing permanently at the Sun. Because of these unique observing conditions and the large active areas of the individual sensors of the CELIAS instrument, measurements can be done with high time resolution and good statistics at the same time.

2 Data Analysis

From the ions recorded with the MTOF sensor, the CELIAS data processing unit accumulates time-of-flight (TOF) spectra for five minutes which then are transmitted to Earth. In this study we evaluated the elements O, Si, and Fe; these three elements are among the most abundant minor ions in the solar wind. Mass peaks for the different elements were extracted from each of the transmitted TOF spectra by fitting the signal and the background with a least square method. Subsequently, the overall efficiency of the MTOF sensor was calculated for each element and for each accumulation interval. To obtain particle fluxes for the chosen elements from the measured count rates, the MTOF sensor response comprising the transmission of the entrance system and the response of the isochronous TOF mass spectrometer (V-MASS) was taken into account.

The settings for the MTOF sensor are cycled in a sequence of six steps, including two voltage settings for the entrance

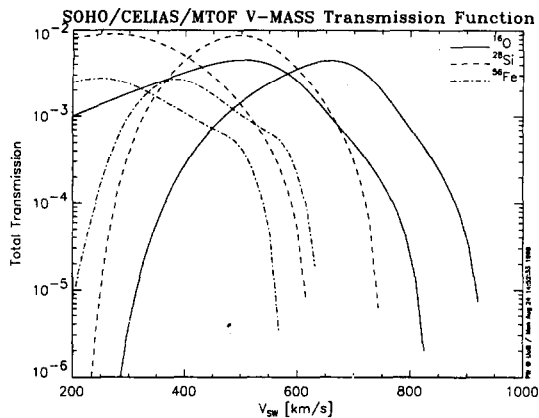


Fig. 1. Total transmission of the isochronous TOF mass spectrometer is plotted for the three elements investigated and for two potential differences between the entrance system and the isochronous TOF mass spectrometer ($V_F = -2500V$ and $V_F = 0V$). The transmissions for $V_F = -2500V$ are peaking at lower solar wind speeds.

system and three values for the potential difference between the entrance system and the TOF mass spectrometer. The potential difference can be either negative, zero, or of positive value, with the negative value accelerating the ions and the positive value decelerating the ions before they enter the TOF mass spectrometer. For the present analysis only the steps with negative and zero potential difference have been used, since the sensor response for the positive potential difference is not known with the required level of confidence yet. In Figure 1 we show the total transmission of the isochronous TOF mass spectrometer for the three elements investigated for negative and zero values of the potential difference between the entrance system and V-MASS. To obtain the total sensor response these numbers have to be multiplied by the response of the entrance system, which is given as an active area (typically $2mm^2$ for a large solar wind speed range). As can be seen from Figure 1, the transmission of the TOF mass spectrometer varies over several orders of magnitude depending on the solar wind conditions and the sensor settings, which complicates the data analysis significantly. The maximum in the V-MASS transmission corresponds to at best 2000 counts for oxygen during a five-minute integration period. The stepping sequence has been optimized to cover a broad range of solar wind conditions. Each step of the MTOF sensor cycle takes five minutes, thus the total sequence takes 30 minutes to finish. However, since each step has quite a large energy bandwidth, overlapping with the other steps considerably, a time resolution of five minutes can be obtained if the sensitivity of the MTOF sensor is high enough for the particular element considered. For typical solar wind conditions and for the more abundant elements in the solar wind, which are studied in this work, it is indeed possible to derive densities with such a high time resolution (Wurz et al., 1998).

The actual solar wind plasma parameters, which were mea-

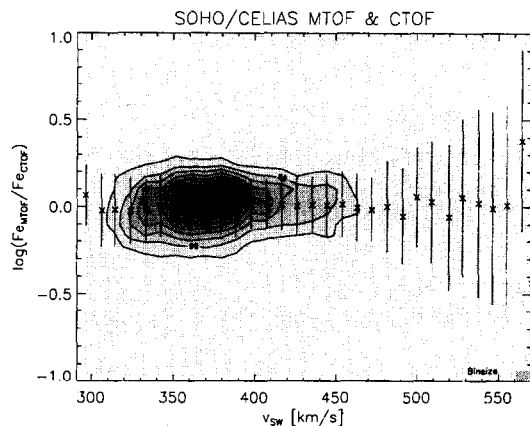


Fig. 2. Logarithm of the ratio of the Fe densities measured with the CELIAS/MTOF sensor versus the Fe densities measured with the CELIAS/CTOF sensor for a time period from day 150 to 229 of 1996 with a total of about 20'000 measurements at 5-minute intervals. The contour lines give the number of measurements for a particular bin. During that time period there was mostly slow solar wind, which explains the clustering of measurements between 350 and 400 km/s. The overlaid symbols are the mean for a particular speed bin and the error bars are the standard deviation of $\log(Fe_{MTOF}/Fe_{CTOF})$ for a single measurement.

sured by the proton monitor (PM), a sub-sensor of the MTOF sensor, are needed as input parameters for the calculation of the MTOF sensor response. The determination of the solar wind plasma parameters with the PM is quite accurate (Ipavich et al., 1998) and better than required for the determination of densities of minor ions with the MTOF sensor.

Another input parameter needed for the determination of the MTOF sensor response, in particular for the determination of the active area of the entrance system, is the charge state distribution of the solar wind ions for each element and for each accumulation interval. The MTOF sensor determines only the mass of the incoming ion. The charge information of the incoming ions is lost because the ions undergo an efficient charge exchange process inside the sensor when they pass the carbon foil of the isochronous TOF mass spectrometer. Therefore, we used the established correlation between the solar wind speed and the freeze-in temperature of the ions (Aellig, 1998; Bochsler, 1997; Hefti, 1997) to derive the so-called freeze-in temperature from the measured solar wind velocity. From the freeze-in temperature we obtained charge state distributions for each element by assuming an ionization equilibrium in the corona and by applying ionization and recombination rates for electronic collisions from Arnaud and co-workers (Arnaud and Rothenflug, 1985; Arnaud and Raymond, 1992). The application of the sensor response to the measured data yielded densities for the different elements.

Since there is still only a limited amount of calibration data available for the MTOF sensor, and since the MTOF sensor response is rather involved, we used the opportunity to compare the oxygen and iron densities we derived from

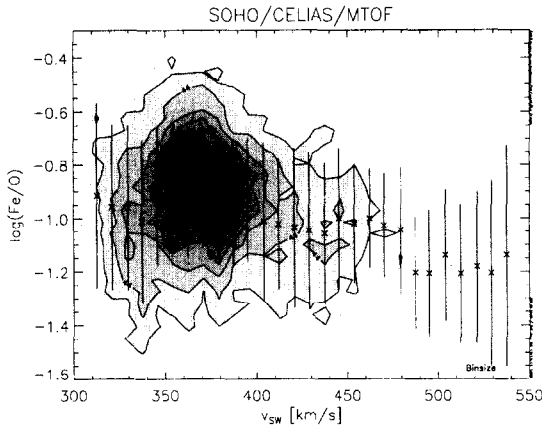


Fig. 3. Logarithm of the Fe/O density ratio measured with CELIAS/MTOF versus the solar wind speed. The 10 linearly spaced contour lines give the number of measurements for a particular bin. During that time period there was mostly slow solar wind which explains the clustering of measurements between 350 and 400 *km/s*. The overlaid symbols are the mean for a particular speed bin and the error bars are the standard deviation of $\log(\text{Fe/O})$ for a single measurement.

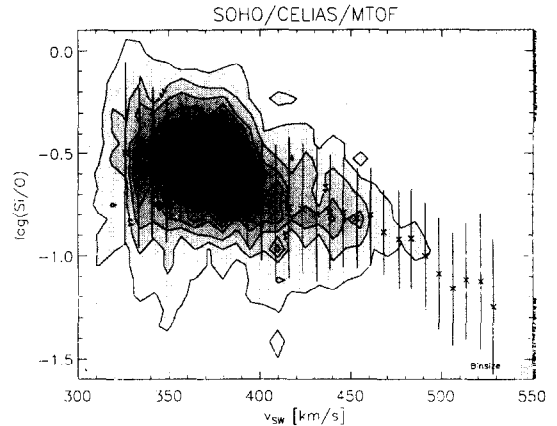


Fig. 4. Logarithm of the Si/O density ratio measured with CELIAS/MTOF versus the solar wind speed. The 10 linearly spaced contour lines give the number of measurements for a particular bin. During that time period there was mostly slow solar wind which explains the clustering of measurements between 350 and 400 *km/s*. The overlaid symbols are the mean for a particular speed bin and the error bars are the standard deviation of $\log(\text{Si/O})$ for a single measurement.

MTOF data with data derived from the CTOF sensor (Aellig, 1998; Hefti, 1997) for the time period for which CTOF data are available (days 150 to 229 of 1996). This comparison is shown in Figure 2 for iron densities, where a total of about 20'000 measurements taken at five-minute intervals are displayed. On average we find good agreement between the two sensors. However, the scattering of individual measurements performed with five-minute time resolution is larger for the MTOF sensor since its overall transmission is significantly lower than the transmission of CTOF, particularly for high solar wind speeds. Furthermore, the range of solar wind speeds which can be investigated is limited at the high solar wind speeds because the transmission becomes very small (see Figure 1). There is no systematic dependence of the instrument function on solar wind speed (shown in Figure 2) and other solar wind plasma parameters like thermal speed, flow direction, measured freeze-in temperature, ... (not shown). For oxygen densities this comparison has also been performed, and we find similar agreement between the two sensors.

3 Results

We evaluated the O, Si, and Fe densities with a time resolution of five minutes for the same time interval for which CTOF data are available. From these density values we derived the abundance ratios Fe/O and Si/O which we analyzed further. We observed strong short-term temporal variations in the density data for the minor ions, significantly stronger than the temporal variation in the proton density data. These findings are in agreement with earlier results reported by Aellig et al. (1998). Also, the abundance ratios Fe/O and Si/O

vary strongly on short time scales of the order of some 10 minutes.

In Figure 3 we show the distribution of Fe/O abundance ratios for the whole time interval, organized by solar wind speed. Clearly, at least two regimes can be identified where the Fe/O abundance ratio is constant: for slow solar wind speeds below 380 *km/s* and for fast solar wind speeds in excess of 480 *km/s*. We associate these solar wind speed regimes with solar wind originating either from the streamer belt regions or the coronal hole regions on the sun, respectively. In between these two regimes we observe a continuous transition from high to low Fe/O abundance ratio which we will discuss later in this paper.

The averaged Fe/O abundance ratios for slow solar wind (< 380 *km/s*) and fast solar wind (> 480 *km/s*), together with published data for the Fe/O abundance ratio, are summarized in Table 1. We find reasonable agreement of our Fe/O abundance ratios with most of the published data, both for the interstream and coronal hole types of solar wind. Only the value reported by Schmid et al. (1988) is considerably higher than other published results and our value, but given the quoted error bar there is no real discrepancy.

In Figure 4 we show the distribution of Si/O abundance ratios for the whole time interval, organized by solar wind speed. Similar to the Fe/O abundance ratio, we again can identify two regimes where the Si/O abundance ratio is constant for an extended solar wind speed interval, for slow solar wind speeds (< 380 *km/s*) and for fast solar wind speeds (> 480 *km/s*). These two regimes are again associated with solar wind originating from streamer belt regions and coronal hole regions on the sun, respectively. The averaged Si/O abundance ratios for these two flow types, together with published

Table 1. Summary of our and reported values for the Fe/O abundance ratio in the solar wind.

Measured regime	Fe/O ratio	Reference
Interstream SW	$0.19^{+0.1}_{-0.07}$	Bochsler <i>et al.</i> (1986); Schmid <i>et al.</i> (1988) ¹⁾
Interstream SW	0.12 ± 0.03	Ipavich <i>et al.</i> (1992)
Interstream SW	0.11 ± 0.03	Aellig <i>et al.</i> (1998) ²⁾
Interstream SW	0.12 ± 0.03	this work
Coronal hole SW	0.057 ± 0.007	Gloeckler <i>et al.</i> (1989)
Coronal hole SW	0.06 ± 0.005	Geiss <i>et al.</i> (1995)
Coronal hole SW	0.063 ± 0.007	this work
Photospheric value	0.0355 ± 0.0025	Anders and Grevesse (1989); Hannaford <i>et al.</i> (1992) ³⁾

¹⁾ This value is a combination of the He/O abundance ratio of 75 from Bochsler *et al.* (1986) and the He/Fe ratio from Schmid *et al.* (1988).

²⁾ The value from Aellig *et al.* (1998) is a weighted average over all solar wind conditions during a three-month time period with mostly slow solar wind.

³⁾ The photospheric value of the Fe/O ratio is derived from the iron abundance given by Hannaford *et al.* (1992) and the oxygen abundance given by Anders and Grevesse (1989).

data for the Si/O abundance ratio, are summarized in Table 2. We find reasonable agreement of our Si/O abundance ratios with the published data, both for the interstream and coronal hole types of solar wind. Between these two regimes where the Si/O abundance ratio is constant we also observe a continuous transition.

4 Discussion

The abundance ratios we find for Fe/O and Si/O are consistent with values reported in the literature (see Tables 1 and 2) for interstream and coronal hole type solar wind. Although the solar wind speed rarely exceeded 500 km/s during the investigated time interval, we can associate this solar wind speed regime with flow from coronal holes extending towards the solar equator since the abundance ratio saturates at a low level consistent with abundance ratio values reported for fast (about 800 km/s) solar wind flow which clearly originated from coronal holes (Geiss *et al.*, 1995; Gloeckler *et al.*, 1989). Recent measurements of elemental abundance in coronal streamers have been performed with SOHO/UVCS by Raymond *et al.* (1997). From these results we derive a Fe/O ratio of $0.13^{+0.05}_{-0.03}$ and a Si/O ratio of $0.05^{+0.02}_{-0.01}$ for the

Table 2. Summary of our and reported values for the Si/O abundance ratio in the solar wind.

Measured regime	Si/O ratio	Reference
Interstream SW	0.19 ± 0.04	Bochsler (1989)
Interstream SW	0.18 ± 0.02	Galvin <i>et al.</i> (1993)
Interstream SW	0.20 ± 0.03	this work
Coronal hole SW	0.054 ± 0.009	Gloeckler <i>et al.</i> (1989)
Coronal hole SW	0.052 ± 0.007	this work
Photospheric value	0.0417 ± 0.0051	Anders and Grevesse (1989)

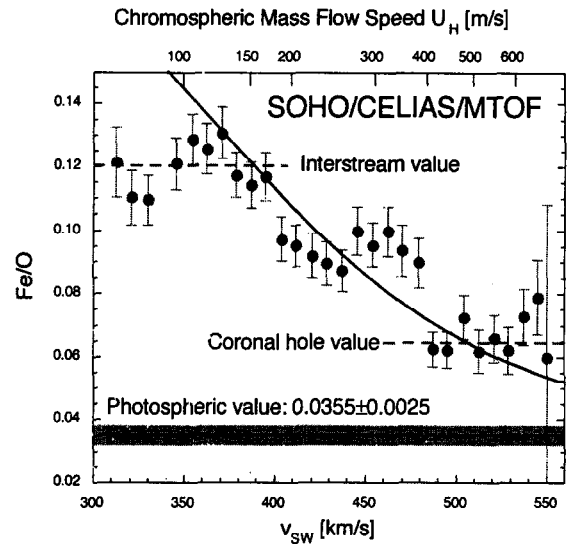


Fig. 5. Average values of the Fe/O ratio for solar wind speed bins of about 10 km/s. The error bars are 1σ errors of the mean plus instrumental uncertainties. The dashed lines indicate the Fe/O ratio reached for slow and fast solar wind, respectively, which are commensurate with published values (see Table 1). The solid line is the result of eq. 1 for a density of $4 \cdot 10^{16} m^{-3}$ and a temperature of $10^4 K$.

leg of an equatorial coronal streamer. The Fe/O value is commensurate with the established abundance ratio for slow solar wind (see Table 1), which is assumed to originate from that location. However, the Si/O value of Raymond *et al.* (1997) is indicative of coronal hole solar wind, which is incompatible with the investigated location. In general the authors observe a depletion of the density of high-FIP elements rather than an enrichment in the density of low-FIP elements at the leg and inside the coronal streamer.

Although silicon and iron are both low FIP elements (the FIPs are 8.15 eV and 7.87 eV, respectively) we observe some differences in the way their elemental abundance relative to oxygen changes for different solar wind regimes. Also the ionization times for silicon and iron are close ($\tau_{Si} = 1.1 s$ and $\tau_{Fe} = 0.91 s$).

Iron behaves like the “classical” low FIP element. Its abundance with respect to oxygen is enriched by a factor of about 4 for interstream solar wind, and by a factor of about 2 for coronal hole type solar wind compared to the photospheric values. Although we did not sample real fast solar wind with speeds around 800 km/s, associated with flow directly from polar coronal holes, we can assume from the leveling off of the Fe/O ratio for solar wind speeds $> 480 km/s$ at the value observed for polar coronal holes (Geiss *et al.*, 1995), that there will not be any further decrease of the Fe/O abundance ratio for higher solar wind speeds than we observed.

For silicon, on the other hand, the FIP fractionation manifests itself somewhat differently from the “classical” FIP picture. For slow solar wind we again observe an enrichment in

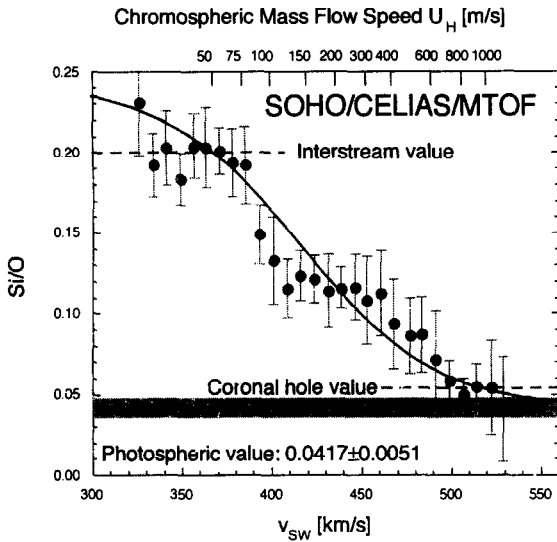


Fig. 6. Average values of the Si/O ratio for solar wind speed bins of about 10 km/s. The error bars are 1σ errors of the mean plus instrumental uncertainties. The dashed lines indicate the Si/O ratio reached for slow and fast solar wind, respectively, which are commensurate with published values (see Table 2). The solid line is the result of eq. 1 for a density of $4 \cdot 10^{16} m^{-3}$ and a temperature of $10^4 K$.

the Si/O ratio of about a factor of four compared to the photospheric ratio. However, for fast solar wind the enrichment in the Si/O ratio compared to the photospheric ratio almost vanishes, i.e., we observe Si/O abundance ratios only marginally higher than the photospheric values in the fast solar wind.

Since we found a clear correlation between the solar wind bulk speed at 1 AU and the elemental fractionation, we tried to compare our results with a recent FIP fractionation model (Peter, 1996), which is the only model using the chromospheric outflow velocities and densities as parameters for the FIP fractionation strength. In this model, which assumes full stationarity of the chromosphere, the FIP fractionation strength is predicted to vary with the chromospheric mass flow speed U_H according to

$$f_{X/O} = \frac{1 + \sqrt{1 + 4(w_X/U_H)^2}}{1 + \sqrt{1 + 4(w_O/U_H)^2}} \quad (1)$$

where w_X are the ionization-diffusion speeds of the ions under consideration ($w_{Si} = 610 m/s$ and $w_{Fe} = 630 m/s$), and $w_O = 105 m/s$ is the ionization-diffusion speed of oxygen, with the respective values adapted from Marsch et al. (1995) for a density of $4 \cdot 10^{16} m^{-3}$. For given conditions in the chromosphere we mapped the chromospheric mass flow speed U_H to the solar wind bulk speed v_{SW} (the proton speed) measured at 1 AU with the PM to account for the observed fractionation values. As we did in an earlier study (Aellig et al., 1998), we used the relationship

$$\log v_{SW} = a + b \log U_H \quad (2)$$

and found that the fractionation we observed can be reproduced by the model by mapping the observed solar wind speed to a chromospheric mass flow speed. In Figures 5 and 6 we show the comparison between the Si/O and Fe/O abundance ratio averages for solar wind speed bins of the data presented above (in Figures 3 and 4) together with the fractionation predicted by eq. 1 for a density of $4 \cdot 10^{16} m^{-3}$ and a temperature of $10^4 K$. These chromospheric parameters were chosen because they are considered typical for the layer in the chromosphere where FIP fractionation process takes place (Geiss and Bochsler, 1986; Marsch et al., 1995). We used a velocity mapping with the parameters in eq. 2 being $a = 2.71$ and $b = 0.114$ for the Si/O ratio and $a = 2.78$ and $b = 0.237$ for the Fe/O ratios. The difference in the parameter b reflects the observed difference in the fractionation for Si/O and Fe/O for fast solar wind. The range of abundance ratios we observe suggests a range of chromospheric mass flow speeds where FIP fractionation occurs. Apparently, the limits for the chromospheric mass flow speeds are given by the heights in the chromosphere where particles enter and exit the fractionation layer, e.g., the location where the density, temperature, and EUV flux (to name just the most important) are in the range necessary for the FIP fractionation. Why the limits of the chromospheric mass flow speeds should be different for Fe/O and Si/O cannot be explained at present. The mapping of the chromospheric mass flow speed to the solar wind speed is a function of the assumed density. Using a lower density results in higher chromospheric mass flow speeds for the same fractionation.

It is generally believed that there is virtually no mass dependence in the FIP effect. The fractionation is mainly governed by the ionization time of the neutral species in the chromosphere and the related diffusion length for the neutrals of the minor species with the dominant hydrogen atoms (Geiss and Bochsler, 1986). Marsch et al. (1995) derived the following asymptotic expression for slow solar wind for the fractionation factor for two species j and k

$$f_{jk} \simeq \frac{r_{kH}}{r_{jH}} \sqrt{\frac{\tau_k}{\tau_j}} \left(\frac{A_j + 1}{A_j} \frac{A_k}{A_k + 1} \right)^{1/4} \quad (3)$$

where f_{jk} is the estimated fractionation factor, r_{iH} the collisional radius of species i with neutral hydrogen, τ_i is the first ionization time, and A_i is the atomic mass of species i . The atomic mass only plays a role in the mobility of the species in a collision-dominated gas and therefore appears only in the fourth root of the mass ratio, slightly favouring the lighter species. However, for transient particle ejection phenomena a mass dependence or a mass per charge dependence in the fractionation of the elements is often found, as has been observed recently for a CME (Wurz et al., 1998).

The stationary assumed in the model by Peter (1996) seems to be a simplification of the actual solar wind flow. As mentioned above, we do see strong short-term fluctuations in the density and the ratio data, which appear to be in conflict with the assumption of stationarity. However, these short-term fluctuations average out when using sufficiently long obser-

vational periods, and by organizing our abundance ratios by solar wind speeds we can indeed compare our data with the model predictions.

5 Conclusions

We find for interstream type solar wind that the Fe/O and Si/O abundance ratios are enriched compared to their photospheric ratios by about a factor of four, which is a typical enrichment for low-FIP elements. In coronal hole type solar wind a reduced FIP effect remains only for Fe but not for Si. Our findings are in good agreement with published results.

Furthermore, we can conclude from our measurements that there are not only two distinct modes of the solar wind, e.g., the slow and the fast solar wind, but there is also a continuous transition between these two extreme cases of solar wind flow, which cannot be explained by simple mixing of two types of solar wind. In case of mixing of two types of solar wind the transition would be much steeper than we measured, which is the result of a Monte-Carlo simulation we performed. These continuous transitions of the abundance ratios with solar wind speeds which we observed, and which have not been seen before, can be explained by the theoretical model of Peter (1996) in which the chromospheric mass flow speed determines the strength of the FIP fractionation process. By mapping the proton speed we observed at 1 AU to the chromospheric mass flow speed, we obtained reasonable agreement between the measured and predicted FIP fractionation. The differences we observe between the two low-FIP elements Si and Fe regarding their FIP fractionation cannot be explained currently. This suggests that the processes involved in the FIP fractionation are more complex than are dealt with in current models.

Acknowledgements. This work is supported by the Swiss National Science Foundation. CELIAS is a joint effort of five hardware institutions under the direction of the Max-Planck Institut für Extraterrestrische Physik (pre-launch) and the University of Bern (post-launch). The Max-Planck Institut für Aeronomie was the prime hardware institution for CTOF, the University of Maryland was the prime hardware institution for MTOF, the University of Bern provided the entrance systems for both sensors, and the Technical University of Braunschweig provided the DPU.

References

- Aellig, M.R., Freeze-in temperatures and relative abundances of iron ions in the solar wind measured with SOHO/CELIAS/CTOF, *PhD Thesis*, University of Bern, Switzerland, 1998.
- Aellig, M.R., S. Hefli, H. Grünwaldt, P. Bochsler, P. Wurz, F.M. Ipavich, D. Hovestadt, The Fe/O elemental abundance in the solar wind, *J. Geophys. Res.*, submitted, 1998.
- Anders, E., and N. Grevesse, Abundances of elements: Meteoritic and solar, *Geochim. Cosmochim. Acta*, 53, 197–214, 1989.
- Arnaud, M., and R. Rothenflug, An updated evaluation of recombination and ionization rates, *Astron. Astrophys. Suppl. Ser.*, 60, 425–457, 1985.
- Arnaud, M., and J. Raymond, Iron ionization and recombination rates and ionization equilibrium, *Astrophys. J.*, 398, 394–406, 1992.
- Bochsler, P., J. Geiss, and R. Joos, Abundances of carbon, oxygen, and neon in the solar wind during the period from August 1978 to June 1982, *Solar Physics*, 102, 177–201, 1986.
- Bochsler, P., Velocity and abundance of silicon ions in the solar wind, *J. Geophys. Res.*, 94 (A3), 2365–2373, 1989.
- Bochsler, P., Particles in the solar wind, *Proceedings of the Fifth SOHO Workshop, ESA SP-404*, 113–122, 1997.
- Galvin, A.B., G. Gloeckler, F.M. Ipavich, C.M. Shafer, J. Geiss, and K. Ogilvie, Solar wind composition measurements by the Ulysses SWICS experiment during transient solar wind flows, *Adv. Space Res.*, 13(6), 75–78, 1993.
- Geiss, J., and P. Bochsler, Solar wind composition and what we expect to learn from out-of-ecliptic measurements, in *The Sun and heliosphere in three dimensions*, R.G. Marsden (ed.), D. Reidel Publishing Company, 173–186, 1986.
- Geiss, J., G. Gloeckler, R. von Steiger, H. Balsiger, L.A. Fisk, A.B. Galvin, F.M. Ipavich, S. Livi, J.F. McKenzie, K.W. Ogilvie, and B. Wilken, The southern high-speed stream: results from the SWICS instrument on Ulysses, *Science*, 268, 1033–1036, 1995.
- Gloeckler, G., F.M. Ipavich, D.C. Hamilton, B. Wilken, W. Stüdemann, G. Kremser, and D. Hovestadt, Heavy ion abundances in coronal hole solar wind flows (abstract), *Eos Trans. AGU*, 70, 424, 1989.
- Hannaford, P., R.M. Lowe, N. Grevesse, and A. Noels, Lifetimes in Fe II and the solar abundance of iron, *Astron. Astrophys.*, 259, 301–306, 1992.
- Hefli, S., Solar wind freeze-in temperatures and fluxes measured with SOHO/CELIAS/CTOF and calibration of the CELIAS sensors, *PhD Thesis*, University of Bern, Switzerland, 1997.
- Hovestadt, D., M. Hilchenbach, A. Bürgi, B. Klecker, P. Laeverenz, M. Scholer, H. Grünwaldt, W.I. Axford, S. Livi, E. Marsch, B. Wilken, P. Winterhoff, F.M. Ipavich, P. Bedini, M.A. Coplan, A.B. Galvin, G. Gloeckler, P. Bochsler, H. Balsiger, J. Fischer, J. Geiss, R. Kallenbach, P. Wurz, K.-U. Reiche, F. Gliem, D.L. Judge, K.H. Hsieh, E. Möbius, M.A. Lee, G.G. Managadze, M.I. Verigin, and M. Neugebauer, CELIAS: The Charge, Element, and Isotope Analysis System for SOHO, *Solar Physics*, 162, 441–481, 1995.
- Ipavich, F.M., A.B. Galvin, J. Geiss, K.W. Ogilvie, F. Gliem, Solar wind iron and oxygen charge states and relative abundances measured by SWICS on Ulysses, *Proceedings of Solar Wind Seven*, E. Marsch and R. Schwenn (eds.), *COSPAR Colloquia Series*, 3, 369–373, 1992.
- Ipavich, F.M., A.B. Galvin, S.E. Lasley, J.A. Paquette, S. Hefli, K.-U. Reiche, M.A. Coplan, G. Gloeckler, P. Bochsler, D. Hovestadt, H. Grünwaldt, M. Hilchenbach, F. Gliem, W.I. Axford, H. Balsiger, A. Bürgi, J. Geiss, K.C. Hsieh, R. Kallenbach, B. Klecker, M.A. Lee, G.G. Managadze, E. Marsch, E. Möbius, M. Neugebauer, M. Scholer, M.I. Verigin, B. Wilken, and P. Wurz, Solar wind measurements with SOHO: the CELIAS/MTOF Proton Monitor *J. Geophys. Res.*, 103 (A8), 17205–17214, 1998.
- Marsch, E., R. von Steiger, P. Bochsler, Element fractionation by diffusion in the solar chromosphere, *Astron. Astrophys.*, 301, 261–276, 1995.
- Peter, H., Velocity-dependent fractionation in the solar chromosphere, *Astron. Astrophys.*, 312, L37–L40, 1996.
- Raymond, J.C., J.L. Kohl, G. Noci, E. Antonucci, G. Tondello, M.C.E. Huber, L.D. Gardner, P. Nicolosi, S. Fineschi, M. Romoli, D. Sparado, O.H.W. Siegmund, C. Benna, A. Ciaravella, S. Cranmer, S. Giordano, M. Karovska, R. Martin, J. Michels, A. Modigliani, G. Naleto, A. Panasyuk, C. Perchele, G. Poletto, P.L. Smith, R.M. Suleiman, and L. Strachan, Composition of coronal streamers from the SOHO ultraviolet coronagraph spectrometer, *Solar Physics*, 175, 645–665, 1997.
- Schmid, J., P. Bochsler, and J. Geiss, Abundance of iron ions in the solar wind, *Astrophys. J.*, 329, 956–966, 1988.
- von Steiger, R., Solar wind composition and charge states, *Proceedings of Solar Wind Eight*, D. Winterhalter, J.T. Gosling, S.R. Habbal, W.S. Kurth, M. Neugebauer (eds.), AIP Press, 193–198, 1996.
- Wurz, P., F.M. Ipavich, A.B. Galvin, P. Bochsler, M.R. Aellig, R. Kallenbach, D. Hovestadt, H. Grünwaldt, M. Hilchenbach, W.I. Axford, H. Balsiger, A. Bürgi, M.A. Coplan, J. Geiss, F. Gliem, G. Gloeckler, S. Hefli, K.C. Hsieh, B. Klecker, M.A. Lee, G.G. Managadze, E. Marsch, E. Möbius, M. Neugebauer, K.-U. Reiche, M. Scholer, M.I. Verigin, and B. Wilken, Elemental composition of the January 6, 1997, CME, *Geophys. Res. Lett.*, 25 (14), 2557–2560, 1998.